Neuron
Article

Contributions of Orbitofrontal and Lateral Prefrontal Cortices to Economic Choice and the Good-to-Action Transformation

Xinying Cai[1] and Camillo Padoa-Schioppa[1,2,3,*]
[1]Department of Anatomy and Neurobiology
[2]Department of Economics
[3]Department of Biomedical Engineering
Washington University in St. Louis, St. Louis, MO 63110, USA
*Correspondence: camillo@wustl.edu
http://dx.doi.org/10.1016/j.neuron.2014.01.008

SUMMARY

Previous work indicates that economic decisions can be made independently of the visuomotor contingencies of the choice task (space of goods). However, the neuronal mechanisms through which the choice outcome (the chosen good) is transformed into a suitable action plan remain poorly understood. Here we show that neurons in lateral prefrontal cortex reflect the early stages of this good-to-action transformation. Monkeys chose between different juices. The experimental design dissociated in space and time the presentation of the offers and the saccade targets associated with them. We recorded from the orbital, ventrolateral, and dorsolateral prefrontal cortices (OFC, LPFCv, and LPFCd, respectively). Prior to target presentation, neurons in both LPFCv and LPFCd encoded the choice outcome in goods space. After target presentation, they gradually came to encode the location of the targets and the upcoming action plan. Consistent with the anatomical connectivity, all spatial and action-related signals emerged in LPFCv before LPFCd.

INTRODUCTION

Recent years witnessed a renewed interest in the neural mechanisms underlying economic choice. Earlier models asserted that all economic decisions unfold as processes of action selection (action-based hypothesis [Glimcher et al., 2005]). However, later results showed that neurons in the orbitofrontal cortex (OFC) encode the identity and subjective value of offered and chosen goods (Padoa-Schioppa and Assad, 2006). In general, a good is defined by a collection of determinants, of which some are external (e.g., commodity, quantity) and others are internal (e.g., motivation) to the subject (Padoa-Schioppa, 2011). Importantly, OFC neurons encode the value of goods independently of the visuomotor contingencies of the choice task. Based on these results and on evidence from lesion studies (Buckley et al., 2009; Camille et al., 2011; Rudebeck and Murray, 2011; West et al., 2011), we proposed that economic decisions generally take place in this abstract representation (good-based hypothesis [Padoa-Schioppa, 2011]). Other authors embraced the notion of good-based decisions (Cisek, 2012; Glimcher, 2011; Rushworth et al., 2012; Wunderlich et al., 2010) but emphasized the importance of motor systems for decision making during the course of evolution (Cisek, 2012; Glimcher, 2011) and the likely involvement of motor systems in decisions under different circumstances (e.g., when offers vary by their action cost [Rangel and Hare, 2010; Rushworth et al., 2012]). Thus, while this topic remains matter of active research, the current consensus is that economic decisions can be made in the space of goods.

In most circumstances, a good-based decision must ultimately guide a suitable action. In other words, the choice outcome must be transformed from goods space to actions space. Thus, to understand choice-guided behavior, it is critical to assess the neural mechanisms of this good-to-action transformation. Notably, central OFC—a brain region where good-based decisions might take place—has no direct anatomical connections with motor structures (Carmichael and Price, 1995). On the other hand, a major anatomical output of the OFC is the ventral portion of lateral prefrontal cortex (LPFCv) (Petrides and Pandya, 2006; Saleem et al., 2013). This region projects to the dorsal portion of lateral prefrontal cortex (LPFCd) (Takahara et al., 2012), which in turn is densely connected with motor systems (Lu et al., 1994; Takada et al., 2004; Takahara et al., 2012). Based on this pattern of anatomical connectivity, we hypothesized that LPFCv/d participate in the early phases of the good-to-action transformation.

To test this hypothesis, we designed an economic choice task that promoted (but did not enforce) good-based decisions. Specifically, we let monkeys choose between different juices offered in variable amounts while we dissociated in space and time the presentation of the offers and the indication of the action associated with each offer. Choices were eventually revealed with an eye movement. Neuronal responses in OFC, which encoded the choice outcome long before the presentation of the saccade targets, indicated that decisions were indeed made in goods space. We thus recorded from LPFCv/d. We found that prior to target presentation, neurons in both these areas encoded the choice outcome in goods space. After target presentation,

neurons in both areas gradually came to encode the spatial location of the saccade targets and, subsequently, the upcoming action plan. This pattern of activity suggests an involvement of these areas in the good-to-action transformation. Consistent with the anatomy, we also found that LPFCv leads LPFCd in the computation of all spatial and action-related signals. While the possible role of other brain regions remains to be assessed, our results suggest that LPFCv/d serve as a key node in the transition from the choice system to motor systems.

RESULTS

Neuronal Evidence for Good-Based Decisions

Monkeys chose between two juices (labeled A and B, with A preferred) offered in variable amounts. Compared to a classic economic choice task (Padoa-Schioppa and Assad, 2006), we dissociated the spatial location of the offers from the saccades necessary to obtain them and we introduced a delay between the presentation of the offers and the saccade targets (Figure 1A). Behavioral choice patterns presented the typical tradeoff between juice type and juice quantity (Figures 1B and 1C). In a control analysis, we verified that choices did not depend on the spatial congruence between the offers and the saccade targets associated with them (see Supplemental Experimental Procedures and Figure S1 available online).

In this study, saccade targets did not indicate the juice amounts and thus did not provide sufficient information to make a decision. Conversely, offers did not provide any information about the saccade necessary to obtain the chosen juice. This experimental design was used to encourage the animal to make decisions in goods space, before planning the action. At the same time, the task design did not necessarily prevent action-based decisions. In particular, the animals could conceivably keep in working memory the two offer values until the saccade targets appeared, attach these offer values to the possible saccades, and finally make their decision in actions space through a process of action selection. To verify that decisions were indeed made in goods space, we examined the activity of neurons in the OFC. We reasoned that neurons encoding the choice outcome (chosen good, chosen value) before saccade targets appear on the monitor would indicate that the decision was indeed abstract from action planning (good based).

We thus recorded the activity of 1,014 cells from the OFC of two monkeys. Neuronal activity was analyzed in nine time windows aligned with different behavioral events: *preoffer* (0.5 s before the offer), *postoffer* (0.5 s after offer on), *late delay* (0.5–1.0 s after offer on), *pretarget* (0.5 s before target on), *posttarget* (0.5 s after target on), *prego* (0.5 s before the "go"), *reaction time* (from "go" to saccade), *prejuice* (0.5 s before the juice), and *postjuice* (0.5 s after the juice). As in previous studies, a neuronal response was defined as the activity of one cell in one time window. Task-related responses (930 in total) were identified with an ANOVA ($p < 0.001$) and submitted to a variable selection analysis (Padoa-Schioppa and Assad, 2006). In essence, we defined a large number of variables that neuronal responses could potentially encode and we performed a linear regression of each response on each variable. Using two independent statistical procedures (stepwise method and best-subset method), we identified a small subset of variables that best explained the neuronal population. Replicating previous results (Padoa-Schioppa and Assad, 2006, 2008) with this new task design, we found that neurons in the OFC encoded three variables: *offer value*, *chosen value* (Figure 1B), and *chosen juice* (Figure 1C). As previously observed, these variables were encoded independently of the spatial configuration of the offers and the direction of the eventual saccade. Most importantly, a substantial fraction of cells encoded *chosen value* and *chosen juice* (i.e., the choice outcome in goods space) in the two time windows following offer presentation, long before saccade targets appeared on the monitor (Figure 1D).

To further verify that decisions were made in goods space, we tested the extent to which the choice outcome could be inferred from *chosen juice* responses recorded prior to target presentation. Consider, for example, the cell in Figure 1C and, specifically, offer types 2B:1A and 3B:1A. The critical question is whether the firing rate recorded in trials in which the animal chose juice A (diamonds) was significantly different from that recorded in trials in which the animal chose juice B (circles). We examined this issue with an ROC analysis. In essence, we compared, for each offer type in which decisions were split, the spike counts recorded for choices of juice A and juice B. For each offer type, we thus obtained an "area under the curve" (AUC). To obtain a single AUC for each response, we averaged the AUC across offer types (Kang and Maunsell, 2012). Thus, AUC was the probability that an ideal observer would successfully infer the decision of the animal from the activity of one *chosen juice* cell. The distribution of AUC obtained across the population is shown in Figure 2A. Notably, mean AUC was significantly higher than chance (mean AUC = 0.625, $p < 10^{-10}$, t test; Figure 2A). This result is particularly significant if one considers the fact that neuronal noise correlations in the OFC are generally low (K. Conen and C.P.-S., unpublished data; Miura et al., 2012). In other words, by looking at the entire population of *chosen juice* cells, an ideal observer would be able to assess with high accuracy the decision of the animal in any particular trial.

One concern might be whether *chosen juice* cells are actually saturated *offer value* cells. In another study (Padoa-Schioppa, 2013), we found that the activity of *offer value* cells was not significantly correlated with the choice of the animal for a given offer type, which would argue against this hypothesis. To further examine this issue, we repeated the analysis of Figure 2A on *offer value* cells. Across the population, the AUC was much smaller than that measured for *chosen juice* cells and did not differ significantly from chance (mean AUC = 0.514, $p = 0.09$, t test; Figure 2B). In conclusion, our analyses demonstrated that decisions were indeed made prior to target presentation and thus in goods space.

Neuronal Activity in Lateral Prefrontal Cortex Reflects the Good-to-Action Transformation

In our study and in many circumstances, economic decisions ultimately lead to suitable actions. Thus, if decisions are made in goods space, through what neuronal mechanisms is the choice outcome transformed into an action plan? Notably, central OFC, the region where neurons encode goods' identities and values (Figure 1E), is interconnected with sensory and limbic regions

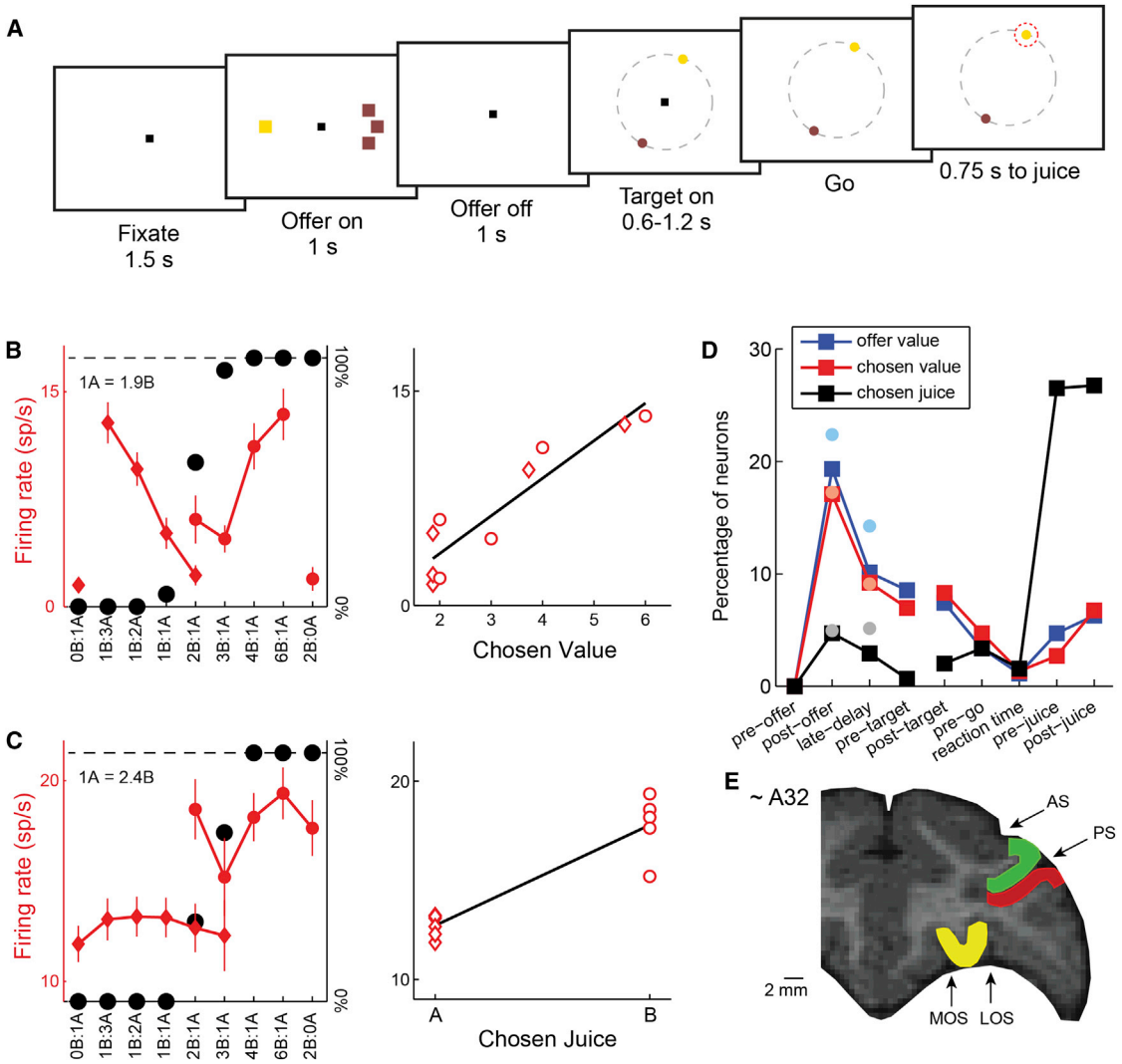

Figure 1. Experimental Design, Recording Locations, and Neuronal Evidence for Good-Based Decisions

(A) At the beginning of the trial, the monkey fixated a center point on the monitor. After 1.5 s, two offers appeared to the left and right of the fixation point. The offers were represented by sets of color squares, with the color indicating the juice type and the number of squares indicating the juice amount. In the trial shown here, the monkey chose between one drop of grape juice (one yellow square) and three drops of tamarind kool-aid (three brown squares). The offers remained on the monitor for 1 s, and then they disappeared. The monkey continued fixating the center point for another 1 s, after which two saccade targets appeared. The location of the saccade targets was randomly selected on a circle (7° radius) centered on the fixation point (eight possible locations), with the two saccade targets on opposite sides of the fixation point. (The circle shown here in gray did not appear on the monitor.) The saccade targets were of different colors corresponding to the colors of the two juices. The monkey maintained fixation for an additional randomly variable delay (0.6–1.2 s) before the center fixation point was extinguished ("go" signal). At that point, the monkey indicated its choice with a saccade. For example, if the animal made a saccade toward the yellow target, it received one drop of grape juice. The monkey then maintained fixation of the target for 0.75 s before juice delivery.

(B) OFC response encoding the *chosen value*. Left: the x axis represents different offer types ranked by ratio #B:#A. Black symbols represent the percentage of "B" choices. Red symbols represent the neuronal firing rate (diamonds and circles for choices of juice A and juice B, respectively; error bars indicate SEM). This neuronal response was recorded in the 0.5 s immediately following the offer (*postoffer* time window). Right: the same neuronal response is plotted against the variable *chosen value* (expressed in units of juice B). The black line is derived from a linear regression.

(C) OFC response encoding the *chosen juice*. This response, encoding the binary choice outcome in goods space, was recorded in the 0.5 s immediately following the offer (*postoffer* time window). All conventions are as in (B).

(D) Time course of encoded variables. Squares indicate the percentage of OFC neurons encoding *offer value*, *chosen value*, and *chosen juice* in different time windows. Faded filled circles show the percentages recorded in a previous study, in which offers and actions were spatially associated and temporally coupled (Padoa-Schioppa and Assad, 2006). Interestingly, the percentage of cells encoding the choice outcome (*chosen value* and *chosen juice*) in the time windows immediately following the offer was statistically indistinguishable between the two studies ($p > 0.3$, χ^2 test).

(E) Recording locations. We recorded from three prefrontal regions: OFC (yellow), LPFCd (green), and LPFCv (red). AS, arcuate sulcus; PS, principal sulcus; MOS, medial orbital sulcus; LOS, lateral orbital sulcus. See also Figure S1.

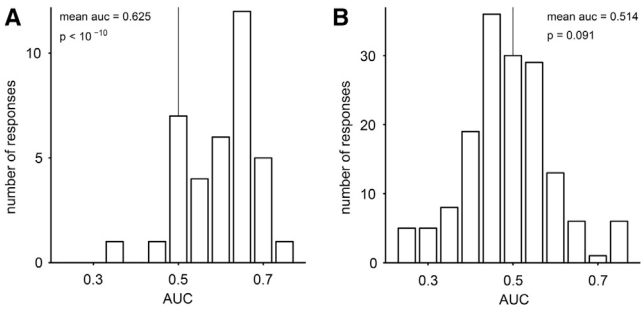

Figure 2. Inferring the Choice Outcome from the Activity of *Chosen Juice* Cells

(A) Distribution of AUC for *chosen juice* responses recorded before target presentation. For each response, we identified the encoded juice as the one eliciting higher activity across all offer types. The ROC analysis focused on offer types in which decisions were split. It compared the neuronal activity for the two groups of trials corresponding to the two choices (we imposed at least five trials for each choice). If a neuronal response had more than one split offer type, AUC was averaged across offer types to obtain one AUC for each response. The distribution of AUC was significantly displaced from chance level (mean AUC = 0.625, $p < 10^{-10}$, t test).

(B) Distribution of AUC for responses encoding the *offer value* before target presentation.

but has vanishingly few connections with motor or premotor regions (Carmichael and Price, 1995). Thus, the good-to-action transformation probably involves multiple steps. To our knowledge, the neural mechanisms of this process have not been investigated previously. In this respect, the lateral prefrontal cortex seems a particularly credible candidate for several reasons. Anatomically, LPFCv receives direct input from central OFC (Petrides and Pandya, 2006; Saleem et al., 2013) and projects to LPFCd, which is connected with multiple motor regions (Lu et al., 1994; Takada et al., 2004; Takahara et al., 2012). Physiologically, neurons in LPFCv/d can encode, in different circumstances, abstract concepts and spatial responses (Genovesio et al., 2005; Miller and Cohen, 2001; Rainer et al., 1998; Tsujimoto et al., 2011; Wallis et al., 2001). To test the role of lateral prefrontal cortex in the good-to-action transformation, we examined the activity of 561 cells from LPFCv and 521 cells from LPFCd (Figure 1E).

What activity pattern would identify a brain area that contributes to the good-to-action transformation? Presumably, neurons involved in this transformation would encode the chosen juice throughout the delay and gradually come to encode the spatial location of the eventual saccade after target presentation. Indeed, we found many neurons with such activity profile. Representative examples from LPFCv and LPFCd are shown in Figures 3A and 3B, where we divided trials in four groups depending on the chosen juice (A or B) and on the cell's preferred hemifield. It can be observed that immediately before target presentation, the cell activity encoded only the chosen juice; after target presentation, however, the neuron gradually came to also encode the saccade direction (hemifield).

Preliminary observations indicated that neurons in LPFCv/d generally multiplex different kinds of signals, including subjective values, juice type, visual, and action-related signals (see Supplemental Experimental Procedures and Figure S2). Consequently, the variable selection analysis used for OFC (where each response encodes only one variable) could not be simply used to examine LPFCv/d. For a quantitative analysis, we thus proceeded as follows. Since neurons in LPFCv/d are spatially selective, their activity after target presentation may depend both on the choice outcome and on the location of the saccade target. In fact, given that two targets appear simultaneously on the monitor, the spatial component can be separated into two factors—whether any target (A or B) appears in the cell's response field, and whether that target is eventually selected as the endpoint of the saccade. To examine these factors separately and quantify how individual neurons reflect them over time, we performed a four-way ANOVA with factors *chosen juice*, *chosen value*, target *orientation* and *hemifield of A*, including all the interaction terms. Importantly, different terms can be interpreted in similar ways (see Experimental Procedures and Table 1). Thus, combining similar terms, the variance of the activity recorded for each neuron can be broken down into six main components: *chosen value*, *chosen juice*, *chosen value* | *juice*, *orientation*, *position of A*, and *chosen target* (see Table 1). This analysis was performed in 100 ms time bins shifted by 25 ms. The results obtained for the two cells illustrated in Figures 3A and 3B provide a proof of concepts (Figures 3C and 3D).

We sought to estimate the variance explained by each ANOVA component at the population level. We noted that the degrees of freedom varied for different components and across cells (depending on the number of trials included in each session). To obviate this problem and to make the results comparable across brain areas, we converted the R^2 of each term into a normalized *Z* score through the following steps. (1) For each cell *i* and each ANOVA component *j*, we estimated the chance level for the corresponding R^2 using a bootstrap procedure. Focusing on a control baseline period (100 ms window starting 500 ms before the offer), we randomly reassigned the spike counts across trials for 1,000 times. We thus obtained a distribution for the baseline R^2, for which we computed the mean ($m_{i,j}$) and SD ($\sigma_{i,j}$). (2) For each cell *i*, each ANOVA component *j*, and each sliding time bin *t*, we converted the R^2 into a *Z* score: $z_{i,j,t} = (R^2_{i,j,t} - m_{i,j})/\sigma_{i,j}$. Thus, for each cell and each component, random fluctuations at chance level had an expected value of 0 and an SD of 1. (3) We then averaged the *Z* scores across the population, separately for each ANOVA component. Note that with a simple population average, random fluctuations at chance level would have an expected value of $\mu_{pop} = 0$ and SD of $\sigma_{pop} = 1/\mathrm{sqrt}(N)$, where N is the number of cells in the population. Thus, to make the results comparable across brain areas (i.e., populations with different number of cells) we normalized the mean:

$$Z_{norm\ j,t} = \sum_{i=0}^{N} z_{i,j,t}/\mathrm{sqrt}\,(N).$$

Hence, for each brain area and for each ANOVA component, Z_{norm} had, at chance level, an expected value of 0 and an SD of $\sigma = 1$.

The results obtained for the population of LPFCv (561 cells; Figure 4A) can be described as follows. During the delay, there was a sustained working memory signal encoding the choice outcome (*chosen value*, *chosen juice*) independent of the

Table 1. Combination and Interpretation of Four-Way ANOVA Components

Term	Component	Interpretation
Chosen value	*Chosen value*	Choice outcome, goods space
Chosen juice	*Chosen juice*	Choice outcome, goods space
Orientation	*Orientation*	Purely visual signal
Hemifield of A	*Position of A*	Purely visual signal
Chosen value × *chosen juice*	*Chosen value* | *juice*	Correlated with offer value
Chosen value × *orientation*	*Bias*	–
Chosen value × *hemifield of A*	*Bias*	–
Chosen juice × *orientation*	*Bias*	–
Chosen juice × *hemifield of A*	*Chosen target*	Action plan
Orientation × *hemifield of A*	*Position of A*	Purely visual signal
Chosen value × *chosen juice* × *orientation*	*Bias*	–
Chosen value × *chosen juice* × *hemifield of A*	*Bias*	–
Chosen value × *orientation* × *hemifield of A*	*Bias*	–
Chosen juice × *orientation* × *hemifield of A*	*Chosen target*	Action plan
Chosen value × *chosen juice* × *orientation* × *hemifield of A*	*Bias*	–

Neuronal data from LPFCv/d were submitted to a four-way ANOVA including all the interactions. The interpretation of each term was as follows. Factors *chosen juice* and *chosen value* capture the choice outcome in goods space. The factor *orientation* captures whether any target is in the cell's response field. Since it does not depend on the color of the target or on the choice of the animal or on the value associated with that target, we interpret it as a purely visual signal. Since there were eight possible target locations and the two targets always appeared in opposite locations, there were four possible orientations. The factor *hemifield of A* specifies whether target A appears on the cell's preferred or antipreferred hemifield. Thus, the interaction *orientation* × *hemifield of A* discriminates which of the two targets (A or B) is in the cell's response field. Since both terms *hemifield of A* and *orientation* × *hemifield of A* can be interpreted as "visual recognition" signals, we combined them in the subsequent analysis (component *position of A*). The three-way interaction *chosen juice* × *orientation* × *hemifield of A* captures the location of the chosen target. The interaction *chosen juice* × *hemifield of A*, which captures the chosen hemifield, is essentially analogous to the three-way interaction, especially if response fields are large (Rainer et al., 1998). We thus combined these two factors in the subsequent analysis (component *chosen target*). Finally, the interaction *chosen value* × *chosen juice* formally represents one aspect of the choice outcome (*chosen value* | *juice*). However, this variable is intrinsically highly correlated with the predecision variable *offer value*, which is not directly present in this analysis. Thus, in our presentation, we conservatively treated *chosen value* | *juice* as a predecision variable. All other interaction terms were negligible in our data sets and were thus combined (component *bias*).

visuomotor contingencies of the task (goods space). Immediately after target presentation, purely visual signals emerged first (components *orientation* and *position of A*), followed by the action planning signal (component *chosen target*). This sequence of signals seems to closely reflect the logical steps of a good-to-action transformation. The analysis of LPFCd provided very similar results (521 cells; Figure 4B). Note that the term *position of A* also captures the interaction between the location of the chosen target and the chosen juice. We performed additional analysis to validate this point (see Supplemental Experimental Procedures and Figure S3).

The curves in Figures 4A and 4B represent the average strength of the effect across the entire population of each area. In a complementary assessment, we quantified for each area the percentage of neurons for which each ANOVA component was statistically significant ($p < 0.01$). The results of this analysis (Figures 4C and 4D) supported the same conclusions obtained based on the analysis of the average strength. As a more conservative measure, we also computed the percentage of neurons based on the F values estimated using a bootstrap procedure and the result was nearly identical to that depicted in Figures 4C and 4D.

Temporal Evolution of Spatial and Action-Related Signals

The results illustrated thus far suggest that both LPFCv and LPFCd participate in the good-to-action transformation. However, known differences between these areas include the anatomical connectivity and physiological properties (Hoshi, 2006; Kennerley and Wallis, 2009; Lebedev et al., 2004; Saleem et al., 2013; Takahara et al., 2012; Yamagata et al., 2012). To compare their possible role, we examined the timing with which spatial and action-related signals emerged in each area. For each cell and for each ANOVA factor, we defined the neuronal latency as the first time in which the normalized R^2 exceeded chance level by 3 SDs ($z_{factor} > 3$) in three consecutive time bins. We then averaged latencies across cells separately for each brain area (Figures 5A and 5B). In both LPFCv and LPFCd, the latencies for *orientation* were significantly shorter than the latencies for *position of A* (LPFCv: $p < 10^{-8}$, LPFCd: $p < 0.01$; Wilcoxon rank-sum test), which in turn were significantly shorter than the latencies for *chosen target* (LPFCv: $p < 10^{-9}$, LPFCd: $p < 10^{-5}$; Wilcoxon rank-sum test). This sequence corresponds to the mental processes presumably undertaken by the animals and is consistent with the interpretation of each ANOVA factor (Table 1). Most strikingly, latencies for each of these three signals were shorter in LPFCv compared to LPFCd. In LPFCv, signals for *orientation*, *position of A*, and *chosen target* appeared on average 156, 203, and 269 ms after target onset. In LPFCd, the same signals appeared on average 208, 236, and 291 ms after target onset. For each ANOVA component, the difference in latency across areas was statistically significant (*orientation*: $p < 10^{-11}$; *position of A*: $p < 0.01$; *chosen target*: $p < 0.01$; Wilcoxon rank-sum test).

One concern in the analysis of neuronal latencies might be that differences between factors or between areas might reflect differences in signal strength. In fact, this is arguably a false issue because the analysis focused on the normalized R^2. Hence, the time at which the signal becomes statistically different from

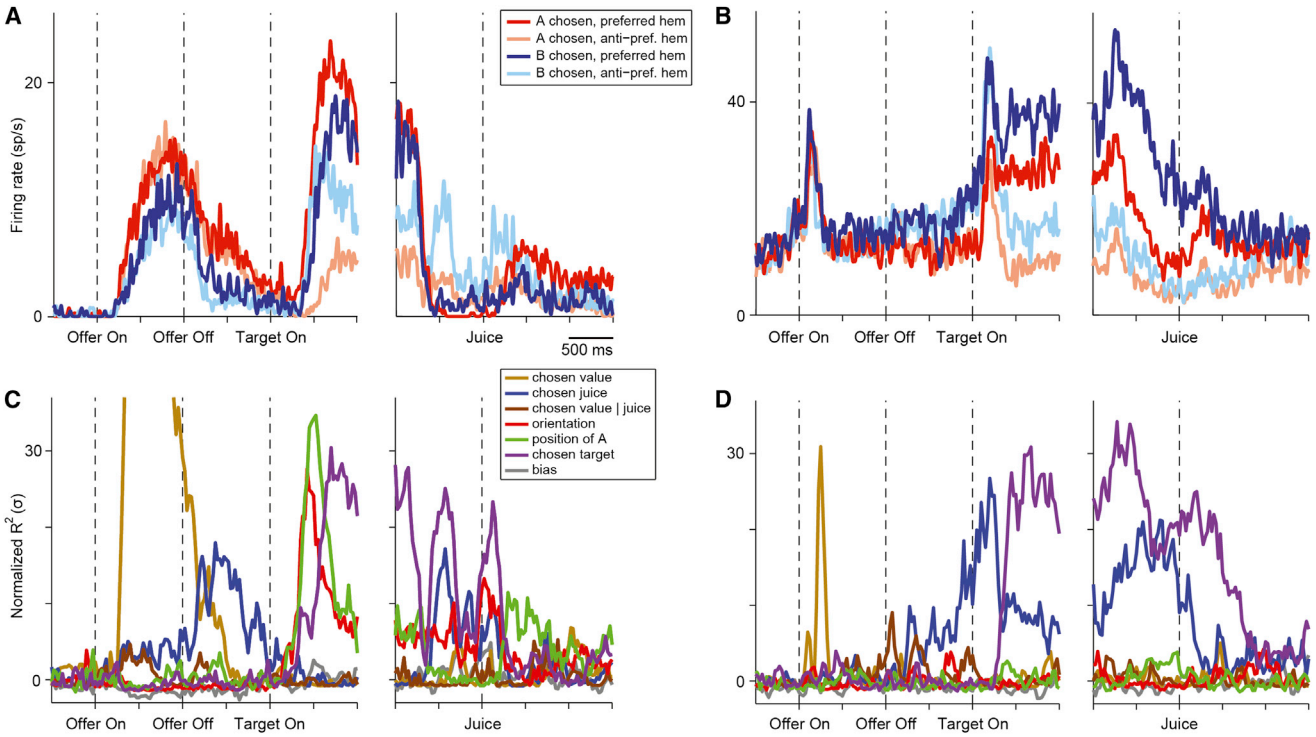

Figure 3. Good-to-Action Transformation, Two Cells

(A) Firing rate of one neuron recorded in LPFCv. Trials were divided in four groups depending on the chosen juice (A or B) and on whether the saccade was directed toward the cell's preferred or antipreferred hemifield (see legend). Immediately before target presentation, the cell activity is modulated by the chosen juice. After target presentation, it gradually comes to also encode the direction of the upcoming saccade (action plan).

(B) One neuron recorded in LPFCd. Same format as in (A).

(C) Results of the four-way ANOVA for the cell shown in (A). ANOVA terms were combined in main components (see legend and Table 1). Because different components had different degrees of freedom, the variance explained by each component was normalized (*Z* scored) compared to a control baseline (see Experimental Procedures). Thus, for each component, the normalized R^2 (y axis) had at chance level an expected value of 0 and an SD of $\sigma = 1$. Immediately before target presentation, the choice outcome term *chosen juice* is the only significant one. The *chosen target* term, reflecting the action plan, emerges after target presentation.

(D) Results of four-way ANOVA for the cell shown in (B). Same format as in (C). See also Figure S2.

chance can be compared across cells irrespective of the eventual peak. In any case, we also examined the distribution of peak times and obtained consistent results (Figures 5C and 5D). In LPFCv, *orientation*, *position of A*, and *chosen target* signals reached their peak on average 254, 280, and 356 ms after target onset. In LPFCd, the same signals reached their peak on average 301, 312, and 385 ms after target onset. For each signal, the peak occurred significantly earlier in LPFCv compared to LPFCd (all $p < 0.01$, Wilcoxon rank-sum test).

For a control, we also examined data from each monkey separately. We found that for each animal, for each ANOVA factor, and for each time measure (latency and peak) the average time was shorter in LPFCv than in LPFCd (12 comparison total). Thus, time differences between the two areas were very robust. In summary, LPFCv leads LPFCd in processing both spatial and action-related signals, suggesting that the LPFCv may be more intimately involved in the early stages of the good-to-action transformation.

Conjunctive Coding of Choice Outcome and Action Plan

We next assessed whether individual neurons conjunctively encoded the choice outcome in goods space and the action plan. More specifically, we examined whether cells that encoded the *chosen juice* immediately before target presentation also encoded the *chosen target* following target presentation.

For this analysis, we focused on large 0.5 s time windows. For each cell and each time window, we repeated the four-way ANOVA and we determined whether a particular component was significantly encoded ($p < 0.01$). For components that included multiple terms (Table 1), we used a Bonferroni correction. We found that cells encoding the *chosen juice* in the pretarget time window were 62/561 (11.0%) in LPFCv and 69/521 (13.2%) in LPFCd. In this respect, the two areas were statistically indistinguishable ($p > 0.2$, z test). Among these neurons, cells encoding the *chosen target* in the subsequent five time windows ranged 34%–69% in LPFCv (Figure 6) and 36%–65% in LPFCd. The percentages obtained for the two areas were statistically indistinguishable in each of the five time windows (all $p > 0.6$, z test). We observed that neurons presenting conjunctive encoding in LPFCd were significantly above chance in all time windows (all $p < 0.01$, χ^2 test). In contrast, the frequency of cells presenting conjunctive encoding in LPFCv did not significantly exceed chance level (five time windows tested, all $p > 0.05$, χ^2 test). As

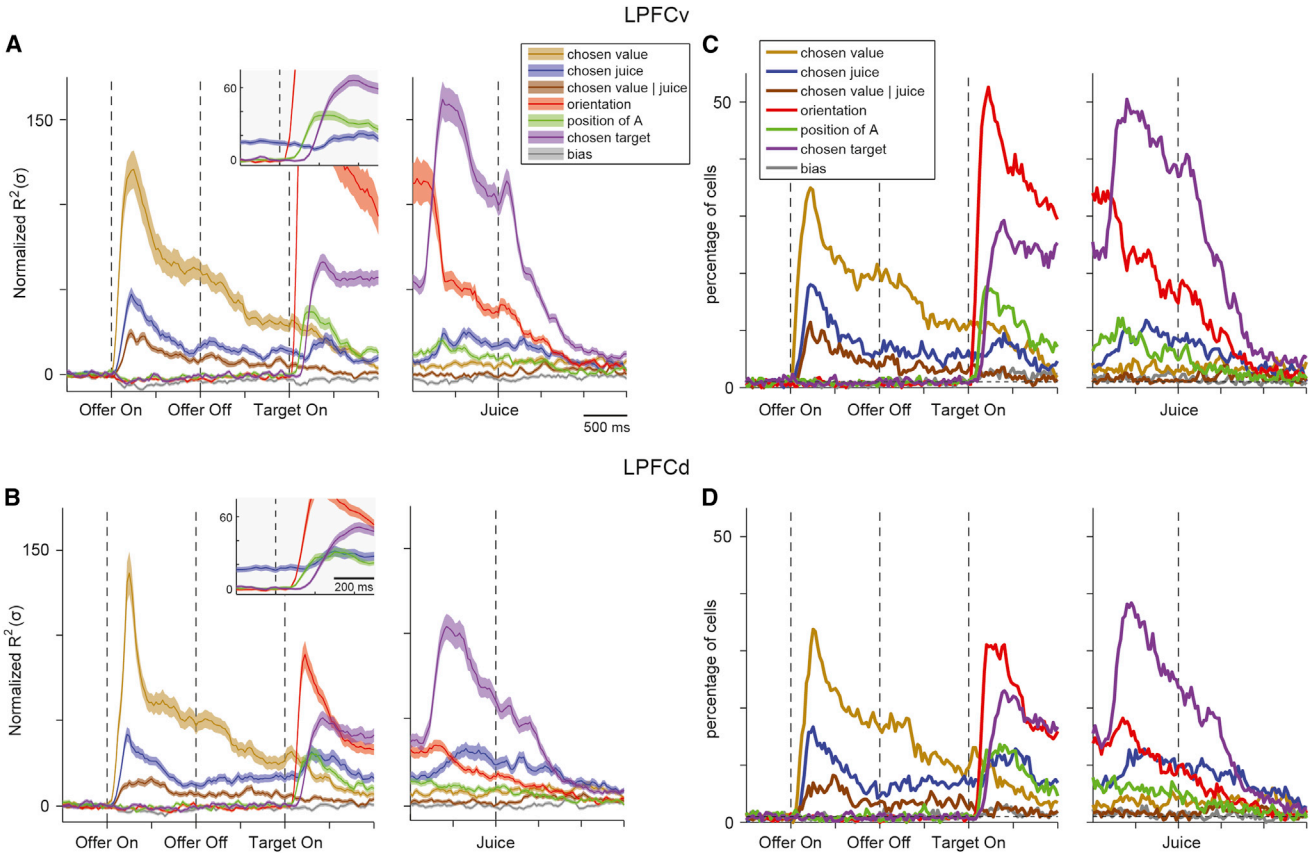

Figure 4. Good-to-Action Transformation, Population Analysis

(A) LPFCv (561 cells). The R^2 obtained for each component of the four-way ANOVA was normalized and averaged across the entire population (see Main Text and Experimental Procedures). The normalized mean R^2 expressed in units of SD (σ; y axis) is plotted here as a function of time (x axis). The insert provides an enlarged view of the window immediately following target presentation (only components relevant to the good-to-action transformation are included). During the delay prior to target presentation, we observed a working memory signal encoding the choice outcome in goods space (*chosen juice*). After target presentation, two purely visual signals (*orientation*, *position of A*) emerged first, followed by the signal representing the upcoming action plan (*chosen target*). The *orientation* component (red, offscale) peaked 175 ms after target on at $Z_{orientation}$ = 162 σ. Shaded areas represent ±SEM.

(B) LPFCd (521 cells). The R^2 for each component was normalized and averaged across the entire population. The results are qualitatively similar to those obtained for LPFCv. All conventions are as in (A).

(C and D) Percentage of neurons encoding different components of the four-way ANOVA in LPFCv (C) and LPFCd (D). Each panel illustrates the percentage of cells for which each component of the four-way ANOVA was significant ($p < 0.01$). For components *position of A* and *chosen target*, each of which is a combination of two terms, we applied a Bonferroni correction when calculating the percentage of cells (we divided the p value in half). The dotted horizontal line indicates chance level (1%). See also Figure S3.

illustrated in Figure 6, this difference between the two areas is essentially due to the fact that cells encoding *chosen target*, but not *chosen juice*, were much more frequent in LPFCv (33%–66%) than in LPFCd (19%–48%).

Neuronal Evidence against a Hybrid Decision Process

The analysis of data from OFC suggests that decisions in this experiment were indeed good based, because neuronal responses encoding the choice outcome (*chosen juice*) were recorded long before target presentation (Figure 1D). One possible concern is whether decisions were actually completed within the space of goods. Indeed, one could entertain a hybrid hypothesis in which the decision is initiated in goods space and finalized in actions space after target presentation (Glimcher, 2011). In this view, the *chosen target* signal recorded in LPFCv/d after target presentation would represent a "decision variable" (Gold and Shadlen, 2001). In analogy to results obtained for perceptual decisions, one might thus predict that the *chosen target* signal depends on the decision difficulty. Specifically, we would expect the *chosen target* signal to emerge more slowly (rapidly) when decisions are harder (easier). The following analysis failed to support this prediction.

In our task, the decision difficulty can be operationally identified with the variable *value ratio* = *other value*/*chosen value* (where *other value* is the value of the nonchosen good). Notably, *value ratio* ≈1 when values are very similar (hard decision) and *value ratio* ≈0 when values are very different (easy decision). For each cell, we thus divided trials into two groups depending on whether the decision was easy or hard, and we repeated the ANOVA separately for the two groups of trials (see

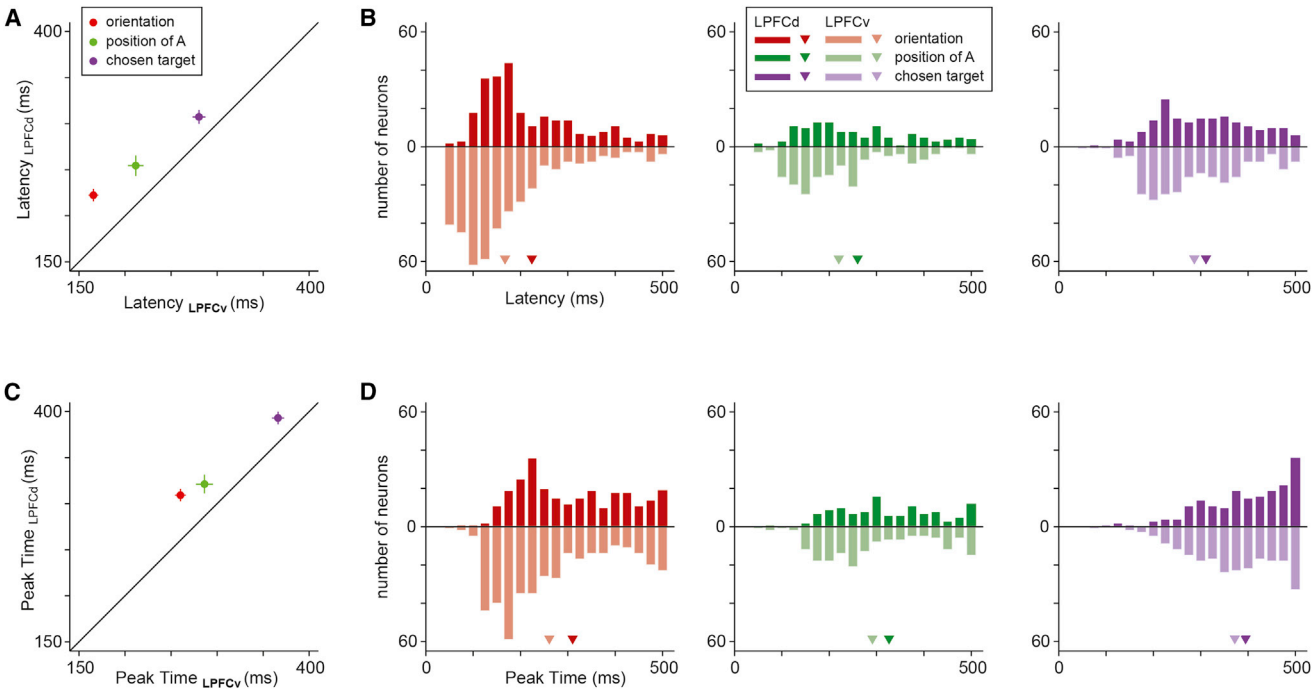

Figure 5. Timing of Spatial and Action-Related Signals

(A) Mean neuronal latencies in LPFCv and LPFCd. In both areas, the latencies for *orientation* were significantly shorter than the latencies for *position of A* (LPFCv: $p < 10^{-8}$, LPFCd: $p < 0.01$; Wilcoxon rank-sum test), which were significantly shorter that the latencies for *chosen target* (LPFCv: $p < 10^{-9}$, LPFCd: $p < 10^{-5}$; Wilcoxon rank-sum test). Error bars indicate SEM. For each signal, the mean neuronal latency in LPFCv was significantly shorter than that in LPFCd (*orientation*: $p < 10^{-11}$; *position of A*: $p < 0.01$; *chosen target*: $p < 0.01$; Wilcoxon rank-sum test).

(B) Distribution of neuronal latencies. Different colors refer to different signals and different areas (see Legend). The triangles indicate mean values.

(C) Mean peak times in LPFCv and LPFCd. For each signal, the mean peak time in LPFCv is significantly shorter than that in LPFCd (all $p < 0.01$, Wilcoxon rank-sum test).

(D) Distribution of peak times.

Experimental Procedures). As observed in Figure 7, the *chosen target* signals measured for the two groups of trials were indistinguishable in both areas. We also performed a statistical analysis of neuronal latencies. For each cell and each group of trials, we defined the *chosen target* latency as the first time in which $z_{chosen\ target} > 3$ in three consecutive time bins. We thus obtained two latency distributions for the two groups of trials. In both areas, neuronal latencies measured for easy decisions were indistinguishable from those measured for hard decisions (both $p > 0.2$, Kolmogorov-Smirnov test; Figure 7, inserts). In conclusion, our analyses argue against the hybrid hypothesis.

DISCUSSION

Lateral Prefrontal Cortex and the Good-to-Action Transformation

Evidence from lesions (Buckley et al., 2009; Camille et al., 2011; Rudebeck and Murray, 2011; West et al., 2011), neurophysiology (Kennerley et al., 2009; O'Neill and Schultz, 2010; Padoa-Schioppa and Assad, 2006; Watson and Platt, 2012), and functional imaging (Chaudhry et al., 2009; Hare et al., 2008; Kable and Glimcher, 2007) suggests that economic choices are based on values computed in the OFC and/or the ventromedial prefrontal cortex (vmPFC) (Kable and Glimcher, 2009; Padoa-Schioppa, 2011; Wallis, 2007). Furthermore, it is generally believed that economic decisions can be made within an abstract representation (Cisek, 2012; Glimcher, 2011; Padoa-Schioppa, 2011; Rushworth et al., 2012; Wunderlich et al., 2010), which might include, in addition to the OFC, vmPFC, the amygdala, parts of the basal ganglia, and possibly other regions. In this study, we examined good-based decisions and we investigated the neuronal process through which the choice outcome, represented in goods space, is transformed into a suitable action plan. We designed a task that dissociated in time decision making from action planning. Prior to target presentation, neurons in OFC and LPFCv/d encoded the chosen good. Shortly after target presentation, neurons in LPFCv/d came to encode the spatial location of the targets and, subsequently, the upcoming action plan. Central OFC, where choice-related signals were found, has no direct connections with motor structures (Carmichael and Price, 1995), but it has major anatomical projections to LPFCv. In turn, LPFCv is connected with motor structures directly and, most prominently, through LPFCd (Lu et al., 1994; Petrides and Pandya, 2006; Saleem et al., 2013; Takada et al., 2004; Takahara et al., 2012). Consistent with this scheme, spatial and action-related signals emerged first in LPFCv, followed by LPFCd. Thus, taken together with the anatomy, our results suggest that neurons in LPFCv/d participate in the early stages of the

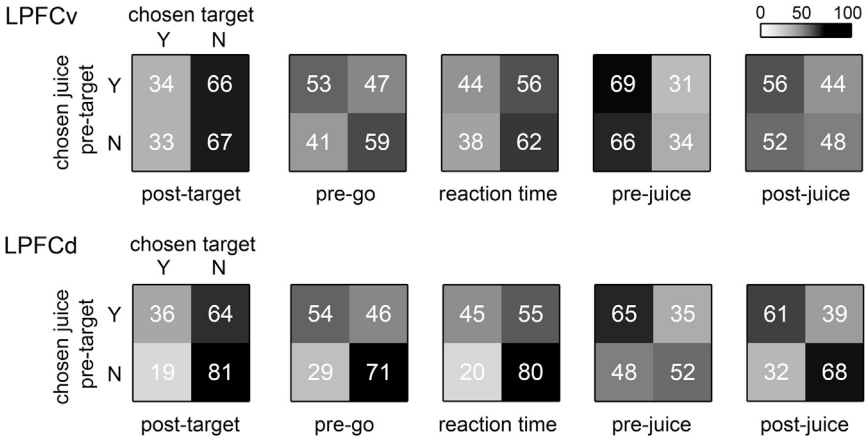

Figure 6. Analysis of Conjunctive Encoding

For each cell and each time window, we determined whether a particular component of the four-way ANOVA was significantly encoded ($p < 0.01$). We thus assessed whether the same cells that encoded the *chosen juice* in the pretarget time window also encoded the *chosen target* after target presentation. Top: of the 561 cells recorded in LPFCv, 62 (499) encoded (did not encode) the *chosen juice* in the pretarget time window. For each time window after target presentation, each of these two groups was divided depending on whether cells encoded the variable *chosen target*. Each panel in the figure illustrates the results of conjunctive coding of *chosen juice* and *chosen target*. Numbers and shades of gray indicate the percent of cells, normalized by the row. For example, considering the leftmost panel, 34% (66%) of cells that encoded the *chosen juice* in the pretarget time window also encoded (did not encode) the *chosen target* in the posttarget time window, whereas 33% (67%) of cells that did not encode the *chosen juice* encoded (did not encode) the *chosen target*. Bottom: LPFCd. Same format as for LPFCv.

good-to-action transformation. However, several questions remain open.

First, it is not clear whether the good-to-action transformation requires LPFCv/d or, alternatively, whether the activity in these areas merely reflects a process that takes place in other brain regions. It is also possible that LPFCv/d are specifically engaged in the transformation only if the choice task includes a delay bridged by working memory, as was the case in the present study. Candidate brain areas that could implement the good-to-action transformation include the dorsal anterior cingulate cortex (ACCd). Indeed, signals encoding choice outcome and movement direction coexist in this area (Cai and Padoa-Schioppa, 2012; Luk and Wallis, 2009). However, we previously observed in ACCd that neuronal activity encoding the *chosen juice* was nearly absent during the decision phase and became prominent only around juice delivery (Cai and Padoa-Schioppa, 2012), too late to contribute to the good-to-action transformation. This fact and the observation that neurons in ACCd encode the choice outcome and the direction of the previous action (Luk and Wallis, 2009) are broadly consistent with the understanding that ACCd is not directly involved in choices between goods and that this area may play a role in associative learning (Alexander and Brown, 2011; Kennerley et al., 2011; Rudebeck et al., 2008). Additionally, it may be noted that anatomical connections between OFC and ACCd are rather indirect and presumably through LPFCv/d. Another candidate region is the tail of the caudate (CDt). A recent study found in CDt neurons tuned to both objects and spatial locations, suggesting that these cells may contribute to orienting the eyes to a particular object in a complex visual environment (Yamamoto et al., 2012). Although these traits resonate with those found here in LPFCv/d, whether neurons in CDt participate in the good-to-action transformation remains to be tested directly. More generally, further work is necessary to examine the possible role of other brain regions in this important process.

Second, each juice in our experiments was associated to a particular color. Thus, the "chosen juice" signals measured in LPFCv/d immediately before target presentation may in fact be related to the chosen color. We cannot rule out this possibility and previous findings would justify either interpretation. Indeed, neurons in this region were found to encode the color of the stimulus when the color was behaviorally relevant (Genovesio et al., 2012). Conversely, in a task designed to make behaviorally relevant the gustatory properties as opposed to the visual properties of the stimulus, the majority of neurons in LPFCv/d encoded the juice taste (Lara et al., 2009). These and other results (Freedman et al., 2001; Nieder et al., 2002; Wallis et al., 2001) underscore the fact that neuronal representations in LPFCv/d are generally malleable to the task demands and do not consistently process the same stimulus attribute. Such malleability arguably facilitates the good-to-action transformation. In general, in any experimental or real-life setting, a good must be pointed to with some label. Here we used color, but labels can in principle be arbitrary. The good-to-action transformation necessarily involves the representation of the proper label. Thus, a brain area that mediates this transformation must be capable of representing arbitrary labels. These considerations motivate the hypothesis that if goods were associated to more complex labels (e.g., different sounds or categories of visual stimuli), neurons in LPFCv/d would generally reflect the transformation from the chosen good/label to the chosen action. This hypothesis shall be tested in future work.

It is also interesting to discuss our results in relation to those obtained in studies of perceptual judgment, where Genovesio et al. (2012) found that neurons in LPFCv/d report the judgment outcome in a domain-general way. In those studies, animals were trained to compare the duration of two stimuli presented sequentially and associated with two colors (red and blue). The color of each stimulus was randomly assigned on a trial-by-trial basis. A substantial population of cells in LPFCv/d encoded the identity of the stimulus (i.e., the color) with a longer duration, especially during the decision and action periods. The authors also compared the activity recorded in two perceptual judgment tasks (discriminating duration and discriminating distance). Neurons in LPFCv/d encoded the identity of the same target stimulus in both tasks (i.e., in a domain-general

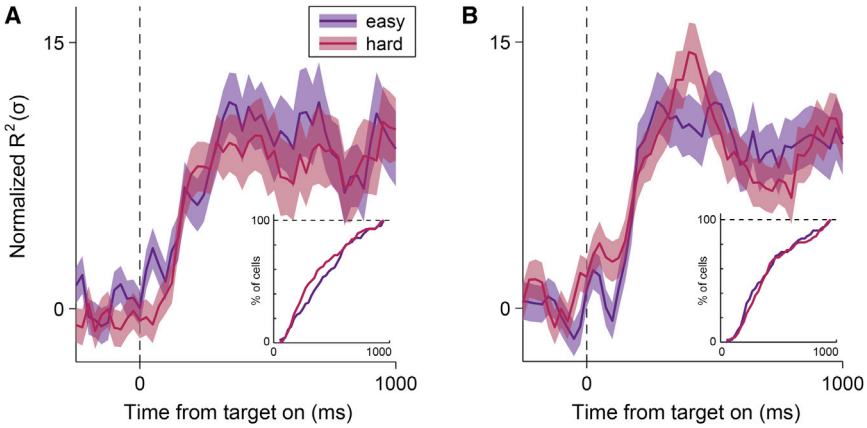

Figure 7. Time Course of *Chosen Target* Signals in Relation to the Decision Difficulty

(A) LPFCv. We examined a hybrid hypothesis in which the decision is initiated in goods space and finalized in actions space after target presentation. Accordingly, we would expect the *chosen target* signal recorded in LPFCv/d to emerge more rapidly when decisions are easy than when decisions are hard. For each cell, we divided trials depending on the decision difficulty. The figure illustrates the time course of the *chosen target* signal separately for the two groups of trials. Contrary to the prediction, the signals obtained in LPFCv for the two groups of trials were very similar. The insert depicts the analysis of neuronal latencies. The distributions obtained for the two groups of trials were statistically indistinguishable ($p > 0.2$, Kolmogorov-Smirnov test; see insert). Shaded areas represent ±SEM.

(B) LPFCd, same analysis as in (A). The distributions of neuronal latencies obtained for the two groups of trials were statistically indistinguishable ($p > 0.7$, Kolmogorov-Smirnov test).

way). Our results suggest that such generality extends not only to different domains of perceptual judgment but also to fundamentally different mental processes—perceptual judgment and economic choice.

Differences between Regions of Lateral Prefrontal Cortex

We observed two differences between LPFCv and LPFCd. First, while the percentage of cells encoding the choice outcome (*chosen juice*) and the action plan (*chosen target*) were comparable in the two areas, neurons encoding only spatial variables were significantly more frequent in LPFCv than in LPFCd. Second, all spatial and action-related signals appeared in LPFCv earlier than in LPFCd. As discussed above, these differences are broadly consistent with the anatomical connectivity. They are also consistent with previous results from neurophysiology and lesion studies. In one experiment, Lebedev et al. (2004) trained monkeys to memorize the original spatial location of a target moving to a new location. Neurons reflecting the attended location, where a target newly appeared, were found more frequently in LPFCv than LPFCd. In another experiment, Rushworth et al. (2005) found that the performance of animals with LPFCv lesions was more severely impaired when the attentional demands of a conditional visuomotor task increased. In a related study, Hoshi and Tanji (2004) found that visual spatial signals in LPFCv lead those in LPFCd. Along similar lines, Kennerley and Wallis (2009) reported that reward-related modulations of spatial signals emerged in LPFCv earlier than that in LPFCd. All these results point to a role of LPFCv in spatial processing and attentional allocation. In contrast, in a study in which monkeys were trained to retrieve two components of information (location of the target and which arm to use) and to integrate them to plan for future action, the proportion of neurons encoding either or both components was significantly higher in LPFCd compared to LPFCv (Hoshi and Tanji, 2004). Thus, one possible interpretation is that the good-to-action transformation involves multiple computational steps, including the allocation of spatial attention followed by the formation of a motor plan. In this view, the timing difference between LPFCv and LPFCd might reflect a differential role of the two areas in these processes.

EXPERIMENTAL PROCEDURES

Animal Preparation and Recordings

Two rhesus monkeys (B, male, 9.0 kg; L, female, 6.5 kg) were used in the experiments. Procedures for surgery, behavioral control, neuronal recordings, and spike sorting were similar to those described previously (Cai and Padoa-Schioppa, 2012; Padoa-Schioppa and Assad, 2006). Briefly, animals sat in an electrically insulated enclosure (Crist Instruments), their head was restrained, and the eye position was monitored with an infrared video camera (Eyelink; SR Research). The behavioral task was controlled through a custom-written software based on MATLAB (MathWorks) and available at http://www.monkeylogic.net/. Structural MRI scans obtained for each animal before and after implant-guided recordings. Tungsten electrodes (125 μm diameter, FHC) were advanced using custom-built motorized microdrives, with a 2.5 μm resolution. We typically used four electrodes in each session. Electrical signals were amplified and band-passed filtered (high pass: 300 Hz, low pass: 6 kHz; Lynx 8, Neuralynx). Action potentials were detected online and saved to disk for subsequent analysis (Power 1,401, Spike 2; Cambridge Electronic Design). All experimental procedures strictly conformed to the NIH *Guide for the Care and Use of Laboratory Animals* and with the regulations at Washington University School of Medicine.

In total, we recorded 1,014 cells from OFC (356 and 658 from monkeys B and L, respectively), 561 cells from LPFCv (362 and 199 from monkeys B and L, respectively), and 521 cells from LPFCd (267 and 254 from monkeys B and L, respectively). Based on the MRI and on the sequence of gray and white matter encountered during electrode penetrations, we identified the region of recordings in OFC as centered on area 13m. For lateral prefrontal cortex, we defined the regions ventral and dorsal to the fundus of the principal sulcus as LPFCv (9/46v) and LPFCd (9/46d), respectively.

Economic Choice Task and Behavioral Analysis

At the beginning of the trial, the monkey fixated a center point on the monitor, within a tolerance window of 2°. (In a small subset of sessions, the tolerance was 3°.) After 1.5 s, two offers appeared to the left and right of the fixation point. The offers were represented by sets of colored squares, with the color indicating the juice type and the number of squares indicating juice amount. The offers remained on the monitor for 1 s, and then they disappeared. The monkey continued fixating the center point for another 1 s. (In a subset of sessions for monkey L, this additional delay lasted only 0.5 s.) At the end of this delay, two saccade targets appeared. The location of the saccade targets

was randomly selected on a circle (7° radius) centered on the fixation point (eight possible locations), with the two saccade targets on opposite side of the fixation point. The color of the saccade targets matched those of the squares representing each offer. The monkey maintained fixation for a randomly variable delay (0.6–1.2 s) before the center fixation point was extinguished ("go" signal), at which point the monkey indicated its choice with a saccade.

All the analyses were conducted in MATLAB. Behavioral data were analyzed as in previous studies (Padoa-Schioppa and Assad, 2006, 2008). Briefly, we expressed choice patterns as a function of log (q_B/q_A), where q_A and q_B are the quantities of juices A and B offered to the monkey, respectively. Each choice pattern was then fit with a normal sigmoid. The underlying Gaussian can be viewed as a distribution of probability for the relative value. The mean of that distribution, corresponding to the flex of the sigmoid, identified the relative value of the two juices.

Variable Selection Analysis and Four-Way ANOVA

The variable selection analysis was conducted as in previous studies (Padoa-Schioppa and Assad, 2006, 2008). We defined nine time windows aligned with different behavioral events. An offer type was identified by two offers (e.g., 1A:3B). A trial type was identified by two offers and a choice (e.g., 1A:3B, A). A neuronal response was defined as the activity of one cell in one time window as a function of the trial type. Task-related responses were identified with a one-way ANOVA (factor trial type, $p < 0.001$) and included in subsequent analyses. We defined 19 variables that neurons in OFC could potentially encode, including value-related variables (*chosen value*, *other value*, *total value*, etc.), juice-specific variables (*offer value A*, *offer value B*, etc.), the binary variable *chosen juice* (previously referred to as *taste* [Padoa-Schioppa and Assad, 2006, 2008]), and number-related variables (*max number*, *total number*, etc.). Each response was regressed on each variable, which was said to explain the response if the regression slope was significantly nonzero ($p < 0.05$). Two methods (stepwise and best subset) were used to identify the subset of variables that best explained the population. As in previous studies, both methods identified *offer value*, *chosen value*, and *chosen juice* as the variables with highest explanatory power. Because the procedures were essentially identical, we could compare the percentage of neurons encoding each variable across studies (see Figure 1D).

A preliminary analysis indicated that neurons in both LPFCv and LPFCd generally carry multiple signals, including subjective values, juice type, and spatial signals. As a consequence, the variable selection analysis used for OFC could not simply be adapted to examine these areas. Indeed that analysis assumes that each neuronal response encodes only one variable. Thus, to examine different factors contributing to the activity of neurons in LPFCv/d, we proceeded as follows. First, we identified for each cell the preferred hemifield using a subset of trials (approximately 20%, with high *chosen value*). We then submitted each cell to a four-way ANOVA with factors *chosen juice*, *chosen value*, *orientation*, and *hemifield of A*, including all the interactions. For this analysis, the factor *chosen value* was reduced to a binary variable, high or low compared to the median. The factor *orientation* was a categorical variable with four levels (since there were eight possible target locations and two targets always appeared in opposite locations, there were four possible orientations). The factor *hemifield of A* was a binary variable depending on whether target A was in the cell's preferred or antipreferred hemifield.

Analysis of Easy versus Hard Decisions

We examined a hybrid model in which the decision is initiated in goods space and completed in actions space after target presentation. If this is the case, the *chosen target* signal recorded in LPFCv/d would be a decision variable, the timing of which would presumably depend on the decision difficulty. Importantly, the timing of the *chosen target* signal can generally depend on multiple factors, including the value of the chosen juice. Thus, to isolate the possible effects of decision difficulty, we proceeded as follows. First, we restricted the analysis to trials in which the monkey chose 1A. Second, we operationally identified the decision difficulty with the variable *value ratio*. Third, we divided trials in two groups depending on the *value ratio* (same number of trials in both groups). Finally, we repeated the ANOVA for the two groups of trials separately. Because the analysis was restricted to choices of 1A, this was a two-way ANOVA with factors *orientation* and *hemifield of A*. The term *chosen target* thus included the term *hemifield of A* and the interaction *orientation* × *hemifield of A*. For a statistical analysis, we defined the neuronal latency as the first time in which $z_{chosen\ target} > 3$ in three consecutive time bins. We thus obtained two latency distributions for the two groups of trials (easy and hard decisions). These distributions were compared with a Kolmogorov-Smirnov test.

SUPPLEMENTAL INFORMATION

Supplemental Information includes Supplemental Experimental Procedure and three figures and can be found with this article online at http://dx.doi.org/10.1016/j.neuron.2014.01.008.

ACKNOWLEDGMENTS

We thank J. Assad, D. Freedman, and L. Snyder for comments on the manuscript. This work was supported by the National Institute on Drug Addiction (grant number R01 DA032758 to C.P.-S.).

Accepted: December 19, 2013
Published: February 13, 2014

REFERENCES

Alexander, W.H., and Brown, J.W. (2011). Medial prefrontal cortex as an action-outcome predictor. Nat. Neurosci. *14*, 1338–1344.

Buckley, M.J., Mansouri, F.A., Hoda, H., Mahboubi, M., Browning, P.G., Kwok, S.C., Phillips, A., and Tanaka, K. (2009). Dissociable components of rule-guided behavior depend on distinct medial and prefrontal regions. Science *325*, 52–58.

Cai, X., and Padoa-Schioppa, C. (2012). Neuronal encoding of subjective value in dorsal and ventral anterior cingulate cortex. J. Neurosci. *32*, 3791–3808.

Camille, N., Griffiths, C.A., Vo, K., Fellows, L.K., and Kable, J.W. (2011). Ventromedial frontal lobe damage disrupts value maximization in humans. J. Neurosci. *31*, 7527–7532.

Carmichael, S.T., and Price, J.L. (1995). Sensory and premotor connections of the orbital and medial prefrontal cortex of macaque monkeys. J. Comp. Neurol. *363*, 642–664.

Chaudhry, A.M., Parkinson, J.A., Hinton, E.C., Owen, A.M., and Roberts, A.C. (2009). Preference judgements involve a network of structures within frontal, cingulate and insula cortices. Eur. J. Neurosci. *29*, 1047–1055.

Cisek, P. (2012). Making decisions through a distributed consensus. Curr. Opin. Neurobiol. *22*, 927–936.

Freedman, D.J., Riesenhuber, M., Poggio, T., and Miller, E.K. (2001). Categorical representation of visual stimuli in the primate prefrontal cortex. Science *291*, 312–316.

Genovesio, A., Brasted, P.J., Mitz, A.R., and Wise, S.P. (2005). Prefrontal cortex activity related to abstract response strategies. Neuron *47*, 307–320.

Genovesio, A., Tsujimoto, S., and Wise, S.P. (2012). Encoding goals but not abstract magnitude in the primate prefrontal cortex. Neuron *74*, 656–662.

Glimcher, P.W. (2011). Foundations of Neuroeconomic Analysis. (Oxford: Oxford University Press).

Glimcher, P.W., Dorris, M.C., and Bayer, H.M. (2005). Physiological utility theory and the neuroeconomics of choice. Games Econ. Behav. *52*, 213–256.

Gold, J.I., and Shadlen, M.N. (2001). Neural computations that underlie decisions about sensory stimuli. Trends Cogn. Sci. *5*, 10–16.

Hare, T.A., O'Doherty, J., Camerer, C.F., Schultz, W., and Rangel, A. (2008). Dissociating the role of the orbitofrontal cortex and the striatum in the computation of goal values and prediction errors. J. Neurosci. *28*, 5623–5630.

Hoshi, E. (2006). Functional specialization within the dorsolateral prefrontal cortex: a review of anatomical and physiological studies of non-human primates. Neurosci. Res. *54*, 73–84.

Hoshi, E., and Tanji, J. (2004). Area-selective neuronal activity in the dorsolateral prefrontal cortex for information retrieval and action planning. J. Neurophysiol. *91*, 2707–2722.

Kable, J.W., and Glimcher, P.W. (2007). The neural correlates of subjective value during intertemporal choice. Nat. Neurosci. *10*, 1625–1633.

Kable, J.W., and Glimcher, P.W. (2009). The neurobiology of decision: consensus and controversy. Neuron *63*, 733–745.

Kang, I., and Maunsell, J.H. (2012). Potential confounds in estimating trial-to-trial correlations between neuronal response and behavior using choice probabilities. J. Neurophysiol. *108*, 3403–3415.

Kennerley, S.W., and Wallis, J.D. (2009). Reward-dependent modulation of working memory in lateral prefrontal cortex. J. Neurosci. *29*, 3259–3270.

Kennerley, S.W., Dahmubed, A.F., Lara, A.H., and Wallis, J.D. (2009). Neurons in the frontal lobe encode the value of multiple decision variables. J. Cogn. Neurosci. *21*, 1162–1178.

Kennerley, S.W., Behrens, T.E., and Wallis, J.D. (2011). Double dissociation of value computations in orbitofrontal and anterior cingulate neurons. Nat. Neurosci. *14*, 1581–1589.

Lara, A.H., Kennerley, S.W., and Wallis, J.D. (2009). Encoding of gustatory working memory by orbitofrontal neurons. J. Neurosci. *29*, 765–774.

Lebedev, M.A., Messinger, A., Kralik, J.D., and Wise, S.P. (2004). Representation of attended versus remembered locations in prefrontal cortex. PLoS Biol. *2*, e365.

Lu, M.T., Preston, J.B., and Strick, P.L. (1994). Interconnections between the prefrontal cortex and the premotor areas in the frontal lobe. J. Comp. Neurol. *341*, 375–392.

Luk, C.H., and Wallis, J.D. (2009). Dynamic encoding of responses and outcomes by neurons in medial prefrontal cortex. J. Neurosci. *29*, 7526–7539.

Miller, E.K., and Cohen, J.D. (2001). An integrative theory of prefrontal cortex function. Annu. Rev. Neurosci. *24*, 167–202.

Miura, K., Mainen, Z.F., and Uchida, N. (2012). Odor representations in olfactory cortex: distributed rate coding and decorrelated population activity. Neuron *74*, 1087–1098.

Nieder, A., Freedman, D.J., and Miller, E.K. (2002). Representation of the quantity of visual items in the primate prefrontal cortex. Science *297*, 1708–1711.

O'Neill, M., and Schultz, W. (2010). Coding of reward risk by orbitofrontal neurons is mostly distinct from coding of reward value. Neuron *68*, 789–800.

Padoa-Schioppa, C. (2011). Neurobiology of economic choice: a good-based model. Annu. Rev. Neurosci. *34*, 333–359.

Padoa-Schioppa, C. (2013). Neuronal origins of choice variability in economic decisions. Neuron *80*, 1322–1336.

Padoa-Schioppa, C., and Assad, J.A. (2006). Neurons in the orbitofrontal cortex encode economic value. Nature *441*, 223–226.

Padoa-Schioppa, C., and Assad, J.A. (2008). The representation of economic value in the orbitofrontal cortex is invariant for changes of menu. Nat. Neurosci. *11*, 95–102.

Petrides, M., and Pandya, D.N. (2006). Efferent association pathways originating in the caudal prefrontal cortex in the macaque monkey. J. Comp. Neurol. *498*, 227–251.

Rainer, G., Asaad, W.F., and Miller, E.K. (1998). Memory fields of neurons in the primate prefrontal cortex. Proc. Natl. Acad. Sci. USA *95*, 15008–15013.

Rangel, A., and Hare, T. (2010). Neural computations associated with goal-directed choice. Curr. Opin. Neurobiol. *20*, 262–270.

Rudebeck, P.H., and Murray, E.A. (2011). Dissociable effects of subtotal lesions within the macaque orbital prefrontal cortex on reward-guided behavior. J. Neurosci. *31*, 10569–10578.

Rudebeck, P.H., Behrens, T.E., Kennerley, S.W., Baxter, M.G., Buckley, M.J., Walton, M.E., and Rushworth, M.F. (2008). Frontal cortex subregions play distinct roles in choices between actions and stimuli. J. Neurosci. *28*, 13775–13785.

Rushworth, M.F., Buckley, M.J., Gough, P.M., Alexander, I.H., Kyriazis, D., McDonald, K.R., and Passingham, R.E. (2005). Attentional selection and action selection in the ventral and orbital prefrontal cortex. J. Neurosci. *25*, 11628–11636.

Rushworth, M.F., Kolling, N., Sallet, J., and Mars, R.B. (2012). Valuation and decision-making in frontal cortex: one or many serial or parallel systems? Curr. Opin. Neurobiol. *22*, 946–955.

Saleem, K.S., Miller, B., and Price, J.L. (2013). Subdivisions and connectional networks of the lateral prefrontal cortex in the macaque monkey. J. Comp. Neurol. Published online November 9, 2013. http://dx.doi.org/10.1002/cne.23498.

Takada, M., Nambu, A., Hatanaka, N., Tachibana, Y., Miyachi, S., Taira, M., and Inase, M. (2004). Organization of prefrontal outflow toward frontal motor-related areas in macaque monkeys. Eur. J. Neurosci. *19*, 3328–3342.

Takahara, D., Inoue, K.I., Hirata, Y., Miyachi, S., Nambu, A., Takada, M., and Hoshi, E. (2012). Multisynaptic projections from the ventrolateral prefrontal cortex to the dorsal premotor cortex in macaques - anatomical substrate for conditional visuomotor behavior. Eur. J. Neurosci. *36*, 3365–3375.

Tsujimoto, S., Genovesio, A., and Wise, S.P. (2011). Comparison of strategy signals in the dorsolateral and orbital prefrontal cortex. J. Neurosci. *31*, 4583–4592.

Wallis, J.D. (2007). Orbitofrontal cortex and its contribution to decision-making. Annu. Rev. Neurosci. *30*, 31–56.

Wallis, J.D., Anderson, K.C., and Miller, E.K. (2001). Single neurons in prefrontal cortex encode abstract rules. Nature *411*, 953–956.

Watson, K.K., and Platt, M.L. (2012). Social signals in primate orbitofrontal cortex. Curr. Biol. *22*, 2268–2273.

West, E.A., DesJardin, J.T., Gale, K., and Malkova, L. (2011). Transient inactivation of orbitofrontal cortex blocks reinforcer devaluation in macaques. J. Neurosci. *31*, 15128–15135.

Wunderlich, K., Rangel, A., and O'Doherty, J.P. (2010). Economic choices can be made using only stimulus values. Proc. Natl. Acad. Sci. USA *107*, 15005–15010.

Yamagata, T., Nakayama, Y., Tanji, J., and Hoshi, E. (2012). Distinct information representation and processing for goal-directed behavior in the dorsolateral and ventrolateral prefrontal cortex and the dorsal premotor cortex. J. Neurosci. *32*, 12934–12949.

Yamamoto, S., Monosov, I.E., Yasuda, M., and Hikosaka, O. (2012). What and where information in the caudate tail guides saccades to visual objects. J. Neurosci. *32*, 11005–11016.

Neuron, Volume *81*

Supplemental Information

Contributions of Orbitofrontal and Lateral Prefrontal Cortices to Economic Choice and the Good-to-Action Transformation

Xinying Cai and Camillo Padoa-Schioppa

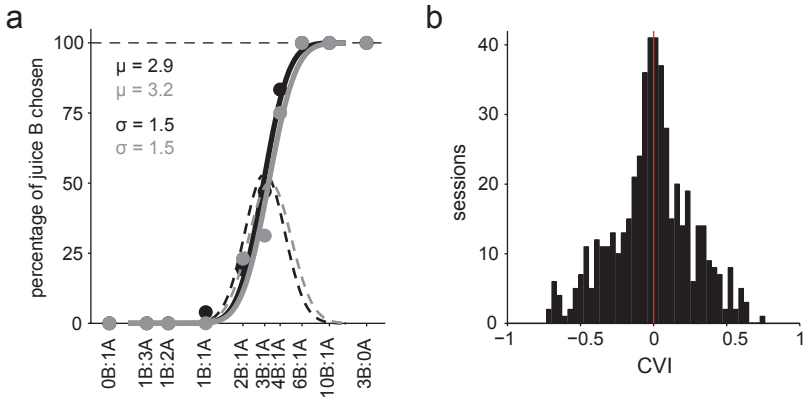

Figure S1. Independence of choice pattern from offer position (related to Figure 1). **a.** One session. Two sets of data points refer to trials in which the position of the chosen offer was in the same (congruent, black) or in the opposite hemifield (incongruent, gray) of that for the chosen target. Continuous lines are fitted sigmoids and dashed lines are the underlying normal distributions. For each fitted sigmoid, the mean (μ) and standard deviation (σ) of the normal distribution provided an estimate and error of measure for the log relative value (see Experimental Procedures). **b.** Distribution of the congruence variability index (CVI) across sessions. If spatial incongruence lead to higher choice variability, CVI would be generally greater than zero. Contrary to this prediction, the distribution of CVI was not significantly displaced from zero (mean CVI = 0.007; p = 0.3, t test).

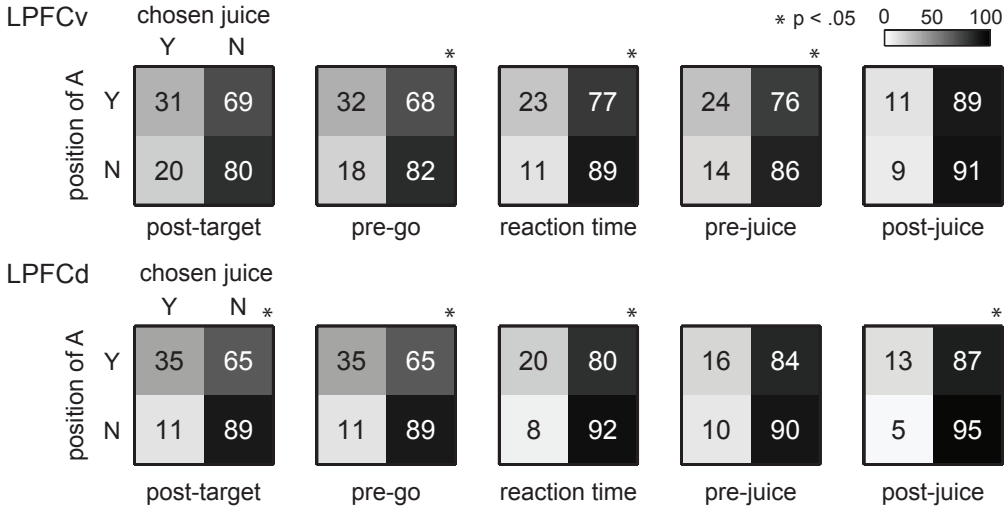

Figure S2. Neurons in LPFCv/d multiplex signals related to juice type and target position (related to Figure 3). For each cell and each time window, we determined whether a particular component of the 4-way ANOVA was significantly encoded ($p<0.01$). We thus assessed whether the same cells that encoded the chosen juice in the pre-target time window also encoded the position of A after target presentation. **Top.** Of the 561 cells recorded in LPFCv, 62 (499) encoded (did not encode) the chosen juice in the pre-target time window. For each time window after target presentation, each of these two groups was divided depending on whether cells encoded the variable position of A. Each panel in the figure illustrates the results of conjunctive coding of chosen juice and position of A. Numbers and shades of gray indicate the percent of cells, normalized by the row. For example, considering the leftmost panel, 31% (69%) of cells that encoded the chosen juice in the pre-target time window also encoded (did not encode) the position of A in the post-target time window, whereas 20% (80%) of cells that did not encode the chosen juice encoded (did not encode) the position of A. **Bottom.** LPFCd. Same format as for LPFCv.

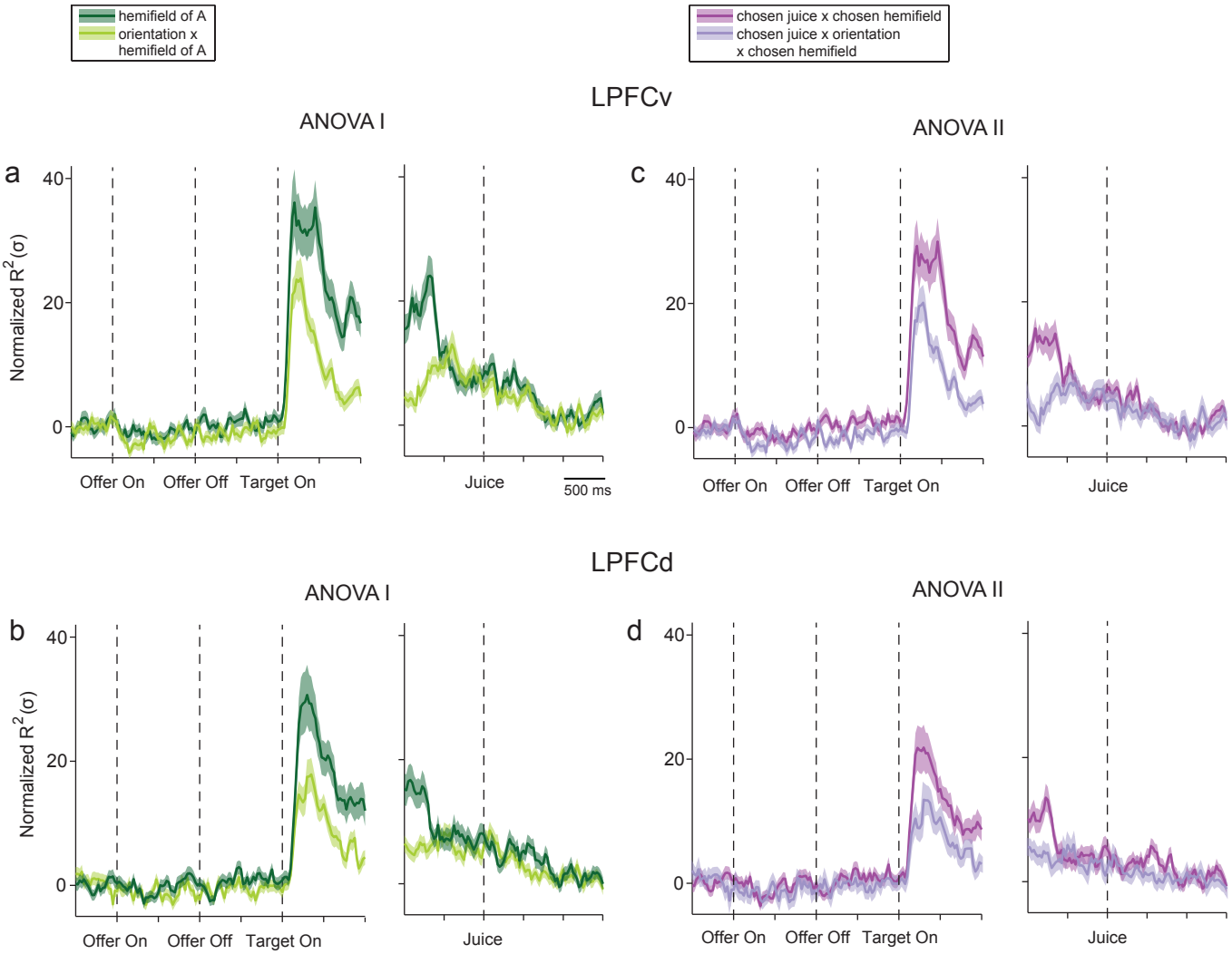

Figure S3. Interaction between chosen targets and chosen juice (related to Figure 4). **a,b.** The two panels labeled "ANOVA I" show, respectively for LPFCv and LPFCd, the results for the same 4-way ANOVA described in the main text analyzing separately the two terms hemifield of A and [orientation x hemifield of A]. In Fig.4, these two terms are combined in the component position of A. **c,d.** The two panels labeled ANOVA II show the results of a 4-way ANOVA with factors chosen value, chosen juice, orientation and chosen hemifield. Here the interaction between chosen juice and chosen target is captured by the following two terms: [chosen juice x chosen hemifield] and [chosen juice x orientation x chosen hemifield]. Note that the temporal profile obtained for hemifield of A in the ANOVA I matches well that of [chosen juice x chosen hemifield] in ANOVA II. This is true for both LPFCv and LPFCd. Likewise, the term [orientation x hemifield of A] in the ANOVA I matches well that of [chosen juice x orientation x chosen hemifield] in ANOVA II.

Supplemental Experimental Procedures

Analysis of behavioral choice patterns: possible effects of spatial congruence

Behavioral data were analyzed as in previous studies (Padoa-Schioppa and Assad, 2006; 2008). Briefly, we expressed choice patterns as a function of $\log(q_B/q_A)$, where q_A and q_B are the quantities of juices A and B offered to the monkey, respectively. Each choice pattern was then fit with a normal sigmoid. The underlying Gaussian can be viewed as a distribution of probability for the relative value. The mean of that distribution, corresponding to the flex of the sigmoid, identified the relative value of the two juices. The sigmoid fit also provided a measure of the choice variability (σ).

For a control, we tested whether the spatial congruence between the offer location and the target location affected the animals' choices. More specifically, we examined whether the choice variability was higher when the left/right location of the chosen offer was spatially incongruent with the chosen target (left/right hemifield). For each recording session (221 sessions for monkey B; 282 sessions for monkey L), we divided trials in two groups depending on whether the chosen offer and chosen target were in the same hemifield (congruent condition) or in opposite hemifields (incongruent condition). We fit the choice patterns for the two groups of trials separately (Fig.S1a) and we obtained the two measures of variability $\sigma_{congruent}$ and $\sigma_{incongruent}$. We then defined the congruence variability index $CVI = (\sigma_{incongruent} - \sigma_{congruent}) / (\sigma_{incongruent} + \sigma_{congruent})$. To test whether the choice variability measured in the incongruent condition was higher than that measured in the congruent condition we submitted the distribution of CVI to a t-test. The result showed that the spatial congruence did not affect the choice variability (Fig.S1b).

Multiplexing of signals related to juice type and target position in the LPFC.

Neurons in LPFCv/d generally multiplex different kinds of signals especially juice type and visual and action-related signals. To illustrate this observation, we performed the analysis of conjunctive encoding examining the *chosen juice* and *position of A* signals from the same time windows after target presentation. As shown in Fig.S2, there was conjunctive encoding of *chosen juice* and *position of A* in most of the time windows after target presentation in LPFCv/d.

Interaction between the spatial location of the chosen target and the chosen juice

In our 4-way ANOVA, the component *position of A* also captures the interaction between the location of the chosen target and the chosen juice. To appreciate this point, consider that this interaction can be broken down in two parts – the interaction [chosen hemifield x chosen juice] and the interaction [chosen target x chosen juice]. In our analysis, the chosen hemifield is represented by the term [*hemifield of A* x *chosen juice*]. Consequently, the first part is [[*hemifield of A* x *chosen juice*] x *chosen juice*] = *hemifield of A*. Similarly, in our analysis, the chosen target is represented by the term [*hemifield of A* x *orientation* x *chosen juice*]. Consequently, the second part is [[*hemifield of A* x *orientation* x *chosen juice*] x *chosen juice*] = [*hemifield of A* x *orientation*]. As detailed in Table 1, the component *position of A* combines these two parts and thus fully captures the interaction. Fig.S3ab illustrates each of these two parts separately.

To validate this point, we performed an additional 4-way ANOVA (referred to as ANOVA II in Fig.S3) with factors *chosen value*, *chosen juice*, *orientation* and *chosen hemifield*. In this formulation, the interaction is quantified directly by the terms [*chosen hemifield* x *chosen juice*] and [*orientation* x *chosen hemifield* x *chosen juice*]. As illustrated in Fig.S3cd, these two terms closely match the terms *hemifield of A* and [*orientation* x *hemifield of A*] of the original ANOVA (referred to as ANOVA I in Fig.S3).